Eur. Phys. J. B **42**, 17–30 (2004)
DOI: 10.1140/epjb/e2004-00354-y

THE EUROPEAN PHYSICAL JOURNAL B

Flow equation approach to heavy fermion systems

K. Meyer[a]

Institut für Theoretische Physik, Technische Universität Dresden, 01062 Dresden, Germany

Received 11 June 2004 / Received in final form 27 September 2004
Published online 26 November 2004 –

Abstract. We use Wegner's flow equation method to investigate the infinite-U periodic Anderson model. We show that this method poses a new approach to the description of heavy fermion behaviour. Within this scheme we derive an effective Hamiltonian in which the c and f degrees of freedom are decoupled. By evaluating one-particle energies as well as correlation functions we find an electronic structure which comprises two gapped quasiparticle bands. We also address the lattice Kondo temperature, which shows a typical exponential dependence on the hybridisation energy. This energy scale exhibits a significant decrease compared to that of the single impurity Anderson model.

PACS. 71.10.Fd Lattice fermion models (Hubbard model, etc.) – 71.27.+a Strongly correlated electron systems; heavy fermions – 75.30.Mb Valence fluctuation, Kondo lattice, and heavy-fermion phenomena

1 Introduction

Heavy fermion systems (HFS) have triggered a growing interest in both experimental and theoretical physics over the last decades. They are mainly based upon lanthanide or actinide compounds, thus their physics is dominated by the interplay of itinerant ($3d$) electrons and rather localised electrons from partly filled $4f$ or $5f$ electron shells. These systems generally posses rich phase diagrams, and they show intriguing physical phenomena, such as superconductivity, long-range magnetic order, Fermi-liquid and non-Fermi-liquid behaviour, and in many cases magnetism and superconductivity coexist. Despite much theoretical effort, many open questions remain even for the paramagnetic metallic phase. At low temperatures this phase is generally characterised by the existence of heavy quasiparticles, which lead to a strongly enhanced specific heat coefficient as well as an enhanced susceptibility. Experiments suggest that the effective mass of the quasiparticles is in the region of several hundreds up to thousand bare electron masses. On a microscopic basis, HFS can be described by the periodic Anderson model (PAM) and the Kondo lattice model (KLM). Whereas the first describes a system of localised f electrons and conduction electrons, which interact via a hybridisation, the latter yields the microscopic picture of a periodic range of magnetic moments in a metallic host. In the so-called Kondo limit the KLM can be regarded as an effective model for the PAM. The physics of both models is associated with the Kondo effect [1], which was initially examined in connection with a single magnetic impurity interacting with a sea of free conduction electrons. The typical energy scale for this interaction is provided by the Kondo temperature T_{K}, which shows an exponential dependence on the hybridisation strength. This relation cannot be understood in terms of conventional perturbation theory. Beside systems that involve f electrons, heavy fermion behaviour has also been observed in LiV_2O_4 [2]. It is believed that the occurrence of a heavy Fermi liquid state is driven by the frustration of the intersite spin couplings [3].

About 10 years ago Wegner [4] and independently Głazek and Wilson [5] proposed a scheme with the objective to diagonalise or block-diagonalise Hamiltonians on the basis of a continuous unitary transformation. This method is known as the flow equation method and has been used for the theoretical description of a great variety of physical systems. In a recent application this method was used to investigate the Hubbard model, a paradigm for a strongly correlated lattice system [6]. Although the authors treated the system on the basis of perturbation theory, they obtained excellent results in the regions of moderate and even strong coupling. In this paper we apply the flow equation method to the infinite-U PAM in order to describe the physics of the paramagnetic metallic phase of HFS. Thereby we do not consider perturbative arguments with respect to the hybridisation strength. We focus on the electronic structure, which suggests the existence of heavy quasiparticles, and show that the lattice Kondo temperature features an exponential dependence on the hybridisation strength. This paper starts off with some general remarks regarding the method and the microscopic model. Afterwards we discuss the application of the method as an approach to the PAM. The last part is devoted to a detailed discussion of our findings.

[a] e-mail: meyer@theory.phy.tu-dresden.de

2 Model and method

2.1 Periodic Anderson model

The PAM is the standard model for the description of heavy fermion systems. Supposing the Coulomb repulsion of the local f electrons being the dominant energy scale in the system, this model can be written in the form

$$H_{\mathrm{PAM}} = \sum_{\mathbf{k}\sigma} \varepsilon_{\mathbf{k}}\, c^{\dagger}_{\mathbf{k}\sigma} c_{\mathbf{k}\sigma} + \sum_{i\sigma} \varepsilon_f\, \hat{f}^{\dagger}_{i\sigma} \hat{f}_{i\sigma} + \frac{1}{\sqrt{N}} \sum_{\mathbf{k}i\sigma} V_{\mathbf{k}} \left(c^{\dagger}_{\mathbf{k}\sigma} \hat{f}_{i\sigma}\, e^{-i\mathbf{k}\mathbf{R}_i} + \hat{f}^{\dagger}_{i\sigma} c_{\mathbf{k}\sigma}\, e^{i\mathbf{k}\mathbf{R}_i} \right). \quad (1)$$

In this representation $\hat{f}^{\dagger}_{i\sigma}$ creates an f electron on site i with spin σ. Due to the infinitely strong Coulomb repulsion of two f electrons doubly occupied sites are explicitly excluded. This is done by the use of Hubbard operators rather than usual fermionic creation and destruction operators:

$$\hat{f}^{\dagger}_{i\sigma} = f^{\dagger}_{i\sigma} \prod_{\sigma'} (1 - n^{f}_{i\sigma'}) = f^{\dagger}_{i\sigma} P^{0}_{i} \quad (2)$$

$$\hat{f}_{i\sigma} = \prod_{\sigma'} (1 - n^{f}_{i\sigma'})\, f_{i\sigma} = P^{0}_{i} f_{i\sigma}. \quad (3)$$

Here $n^{f}_{i\sigma}$ denotes the number operator for the f electrons. The essential property of the Hubbard operators is that the creation operator $\hat{f}^{\dagger}_{i\sigma}$ only acts on an empty site i, and the operator $\hat{f}_{i\sigma}$ only annihilates a singly occupied state. The operator P^{0}_{i} stands for the projector on the empty f site i. In this context the physical subspace merely comprises singly occupied and empty f-sites. As a consequence the completeness relation $P^{0}_{i} + \sum_{\sigma} \hat{f}^{\dagger}_{i\sigma} \hat{f}_{i\sigma} = \mathbf{1}$ holds, and the operators obey the following anti-commutation relations

$$\left\{ \hat{f}^{\dagger}_{i\sigma}, \hat{f}_{i'\sigma'} \right\}_{+} = \delta_{ii'} \left(\delta_{\sigma\sigma'}\, \hat{f}_{i\sigma} \hat{f}^{\dagger}_{i\sigma} + \hat{f}^{\dagger}_{i\sigma} \hat{f}_{i\sigma'} \right). \quad (4)$$

The Fourier transform of the Hubbard operators can be defined in the usual way as $\hat{f}^{\dagger}_{\mathbf{k}\sigma} = 1/\sqrt{N} \sum_i \exp(i\mathbf{k}\mathbf{R}_i) \hat{f}^{\dagger}_{i\sigma}$, where N is the number of lattice sites. However, the above introduced commutation relations for the Hubbard operators in the local picture result in rather complex commutation relations for the operators $\hat{f}^{\dagger}_{\mathbf{k}\sigma}$ and $\hat{f}_{\mathbf{k}\sigma}$. In equation (1) $c^{\dagger}_{\mathbf{k}\sigma}$ creates a conduction electron with momentum $\mathbf{k}$ and spin σ. Whereas the f electrons are localised, the conduction electrons possess a dispersion $\varepsilon_{\mathbf{k}}$. The two subsystems are connected via a hybridisation of the strength $V_{\mathbf{k}}$. Although, in general, a dispersive hybridisation may be examined, we here focus on the case $V_{\mathbf{k}} = \text{const.}$, i.e. an interaction which is restricted to electrons on the same lattice site only. As a further simplification we only consider a hybridisation between c and f electrons within the same spin channel.

The model (1) has been in the focus of a great variety of theoretical investigations. One of the most descriptive ones is the slave-boson mean-field (SBMF) theory [7]. Here the Hubbard operators are treated by the introduction of auxiliary boson fields, which ensure the conservation of the commutation relations. On the other hand, the configuration space of the particles must be restricted due to their bosonic character. This can be accomplished by considering the constraint with the help of additional couplings in the Hamiltonian. The used Lagrange multipliers have to be determined self-consistently. For this model the problem can be solved in the limit $\nu_f \to \infty$, where the latter quantity denotes the spin degeneracy of the f orbitals. A quite similar treatment of the model is provided by the Gutzwiller variational method [8], which can also be formulated in terms of auxiliary bosons [9]. The intriguing result of this approach is an instability of the ground state with respect to ferromagnetic ordering for the case $\nu_f = 2$, and the Kondo temperature is significantly enhanced compared to the single impurity case.

Though the analytical approaches to the PAM have given insight to various aspects of heavy fermion systems, they generally have to deal with more or less rude simplifications. In the last decade a range of numerical solutions emerged. A great number of recent works are based on the Dynamical mean-field theory (DMFT) [10]. Here the PAM can be mapped onto an effective single impurity Anderson model (SIAM). This approach proves to be exact in infinite dimensions, and it is considered to deliver good results even for three-dimensional systems. The major task of this scheme is a self-consistent numerical solution of the impurity problem, whereby a number of methods, such as Wilson's numerical renormalisation group (NRG) [11], Quantum Monte Carlo (QMC) simulations [12] and iterated perturbations theory (ITP) [13], have been used. Other numerical approaches comprise the diagonalisation of small clusters [14] and QMC [15] for the full system. As the numerical results of Section 5 are obtained for a one-dimensional system, we should mention that this system and the corresponding KLM have been extensively studied in the framework of the Density Matrix Renormalisation Group (DMRG) [16]. Various studies of the KLM suggest this system being in the universality class of Luttinger liquids. The phase diagram of the one-dimensional PAM was subject of a series of recent works [17].

Some basic properties of the model equation (1) have also been discussed in the framework of a renormalisation approach by Becker et al. [18], which incorporates the use of hard cut-off functions. However, the authors use perturbation theory with respect to the hybridisation strength and neglect processes that connect different f sites, which is not sufficient to obtain the proper heavy fermion behaviour.

2.2 Flow equation method

The flow equation method is based on the formulation of a continuous unitary transformation. For this reason in various works this approach is referred to as CUT. The transformation is represented by a unitary Operator $U(\ell)$, for a given Hamiltonian H. Here ℓ denotes the flow parameter [19] and the according transformed Hamiltonian is

simply given by $H(\ell) = U(\ell)HU^\dagger(\ell)$. By definition the operator $U(1)$ stands for the identity operator and the fully transformed Hamiltonian $H(\ell = \infty)$ is written as H^*. The latter may be regarded as an effective Hamiltonian, and due to the unitarity of the mapping it possesses the same system of eigenenergies as H. The flow of $H(\ell)$ can be conveniently formulated in its differential representation

$$\frac{\mathrm{d}H(\ell)}{\mathrm{d}\ell} = \big[\eta(\ell), H(\ell)\big] \tag{5}$$

and it is governed by the generator

$$\eta(\ell) = \frac{\mathrm{d}U(\ell)}{\mathrm{d}\ell}U^\dagger(\ell) = -\eta^\dagger(\ell). \tag{6}$$

This operator can be chosen to map H onto a much simpler Hamiltonian. If one starts out, for instance, with a Hamiltonian of the structure $H = H_0 + H_1$, where H_0 represents a system of free particles and H_1 an interaction, the choice

$$\eta = \big[H_0, H_1\big] \tag{7}$$

indeed triggers the interaction part to vanish in the limit $\ell \to \infty$. This can be proved by some simple calculation and equation (7) represents the original choice of the generator by Wegner [4]. In this context the resulting effective Hamiltonian is diagonal or block-diagonal. Beside Wegner's generator, in the recent years a variety of diverse generators has been used. As we have mentioned in the introductory section, an independent approach formulated by Głazek and Wilson was made, in which the Hamiltonian is diagonalised by integrating out higher energy contributions. Another choice for the generator was proposed by Knetter and Uhrig [20]. It has the intriguing feature that it allows the construction of a particle-number conserving effective Hamiltonian.

Independent of the choice of any particular generator, the transformation can as well be applied to formulate the flow of observables. Similar to the structure we have derived for the Hamiltonian, an arbitrary operator is transformed as

$$\frac{\mathrm{d}A(\ell)}{\mathrm{d}\ell} = \big[\eta(\ell), A(\ell)\big]. \tag{8}$$

As a result of this we can take advantage of the invariance of expectation values and correlation functions under unitary transformations. In this sense these quantities can be evaluated with respect to the much simpler Hamiltonian H^* by the simultaneous transformation of the operators. If we regard for example the expectation value of an observable A, the relation

$$\langle A\rangle = \frac{\mathrm{Tr}Ae^{-\beta H}}{Z} = \frac{\mathrm{Tr}A^*e^{-\beta H^*}}{Z} \tag{9}$$

holds, where Z is the partition function.

The above considerations are instructive for the evaluation of Green's functions. If we address, for instance, the retarded Green's function $\langle\langle A(t); B(t')\rangle\rangle = -i\theta(t - t')\langle\{A(t), B(t')\}_+\rangle$, we can use the fact that these quantities are invariant with regard to a unitary transformation. This allows us to evaluate the expectation value and the Heisenberg time dependence of the operators with respect to the transformed Hamiltonian H^*, if we use the transformed operators A^* and B^* at the same time. In terms of the Fourier transformed Green's function this can be simply denoted as $\langle\langle A; B\rangle\rangle(\omega + i\delta) = {}^*\langle\langle A^*; B^*\rangle\rangle^*(\omega + i\delta)$.

3 Flow equations for the periodic Anderson model

After having discussed the general aspects of the model and the method we now focus on the application of the flow equation approach to the infinite-U PAM. This section is organised as follows. First we introduce an appropriate generator with the objective to map the model onto a much simpler one, and subsequently we discuss the flow of the Hamiltonian. In a second step the transformation of observables is examined and the evaluation of expectation values is discussed. The last part of this section then is devoted to the solution of the resulting flow equations.

3.1 Flow of the Hamiltonian

As we have mentioned in the introductory remarks regarding the flow equation method an appropriate choice of the generator is provided by (7). The aim of our treatment of the PAM is the decoupling of the distinct types of electrons, namely the c electrons and the f electrons. They are connected by a hybridisation which is characterised by the energy $V_{\mathbf{k}}$. If we identify this contribution with the interacting part of the Hamiltonian, we recognise that the remaining contribution is not diagonal in the usual sense. This is due to the representation of the f electrons by Hubbard operators and results from the incorporation of their strong Coulomb interaction. Consequently, we use for the generator the more general form

$$\eta(\ell) = \sum_{\mathbf{k}\sigma} \eta_{\mathbf{k}}(\ell)\,\big(c^\dagger_{\mathbf{k}\sigma}\hat{f}_{\mathbf{k}\sigma} - \hat{f}^\dagger_{\mathbf{k}\sigma}c_{\mathbf{k}\sigma}\big). \tag{10}$$

The coefficient $\eta_{\mathbf{k}}$ has to be determined later. A similar definition has already been used for the flow equations analysis of related models [21,22].

A first remarkable result of the above choice for the generator is the generation an f electron hopping of the form

$$H_{ff} = \sum_{i\neq j\sigma} t_{ij}(\ell)\,\hat{f}^\dagger_{i\sigma}\hat{f}_{j\sigma} \tag{11}$$

as a consequence of the evaluation of the commutator in equation (5). A detailed discussion of all contributions is given below. The dispersion of the $f$electrons is obtained by the Fourier transform of the hopping matrix element t_{ij} with the exclusion of local processes

$$\Delta_{\mathbf{k}}(\ell) = \frac{1}{N}\sum_{i\neq j} t_{ij}(\ell)\,e^{-i\mathbf{k}(\mathbf{R}_i - \mathbf{R}_j)}. \tag{12}$$

With this additional interaction term the Hamiltonian of the flow results in the following form:

$$H_{\mathrm{PAM}}(\ell) = \sum_{\mathbf{k}\sigma} \varepsilon_{\mathbf{k}}(\ell)\, c^\dagger_{\mathbf{k}\sigma} c_{\mathbf{k}\sigma} + \sum_{\mathbf{k}\sigma} \big(\varepsilon_f(\ell) + \Delta_{\mathbf{k}}(\ell)\big)\, \hat{f}^\dagger_{\mathbf{k}\sigma} \hat{f}_{\mathbf{k}\sigma} + \sum_{\mathbf{k}\sigma} V_{\mathbf{k}}(\ell)\, \big(c^\dagger_{\mathbf{k}\sigma} \hat{f}_{\mathbf{k}\sigma} + \hat{f}^\dagger_{\mathbf{k}\sigma} c_{\mathbf{k}\sigma}\big) + E(\ell). \quad (13)$$

Besides the hopping of the f electrons an additional energy shift $E(\ell)$ was introduced.

As a general convention for the upcoming considerations we suppress the explicit declaration of the ℓ-dependence of all energies. We only use it in some cases in order to avoid confusions. Furthermore, we use for a certain quantity Q the representation Q^{i} for its initial value, i.e. $Q(\ell = 0)$, and Q^* for the limit $\ell \to \infty$.

Equation (5) poses the central relation of the flow equation method, thus our task is the evaluation of the commutator of the generator (10) and the Hamiltonian (13). As the scheme suggests the resulting contributions determine the flow of the Hamiltonian. The commutator can be easily calculated by making use of the commutator relation (4) for the Hubbard operators. By doing so we arrive at the following result:

$$\begin{aligned}\big[\eta, H\big] = &- \sum_{\mathbf{k}\sigma} \eta_{\mathbf{k}} \left(\varepsilon_{\mathbf{k}} - \varepsilon_f\right) \left(c^\dagger_{\mathbf{k}\sigma} \hat{f}_{\mathbf{k}\sigma} + \hat{f}^\dagger_{\mathbf{k}\sigma} c_{\mathbf{k}\sigma}\right) \\ &+ \frac{1}{\sqrt{N}} \sum_{\mathbf{k}\sigma} \sum_{i\neq j} \eta_{\mathbf{k}}\, t_{ij}\, e^{-i\mathbf{k}\mathbf{R}_i} P^0_i c^\dagger_{\mathbf{k}\sigma} \hat{f}_{j\sigma} + \mathrm{h.c.} \\ &+ \frac{1}{\sqrt{N}} \sum_{\mathbf{k}\sigma\sigma'} \sum_{i\neq j} \eta_{\mathbf{k}}\, t_{ij}\, e^{-i\mathbf{k}\mathbf{R}_i} \hat{f}^\dagger_{i\sigma'} \hat{f}_{i\sigma} c^\dagger_{\mathbf{k}\sigma} \hat{f}_{j\sigma'} + \mathrm{h.c.} \\ &+ \frac{1}{N} \sum_{\mathbf{k}\mathbf{k}'} \sum_{i\sigma} e^{i(\mathbf{k}'-\mathbf{k})\mathbf{R}_i}\, \eta_{\mathbf{k}} V_{\mathbf{k}'}\, c^\dagger_{\mathbf{k}\sigma} c_{\mathbf{k}'\sigma} P^0_i + \mathrm{h.c.} \\ &- \frac{1}{N} \sum_{\mathbf{k}\mathbf{k}'} \sum_{i\sigma\sigma'} e^{i(\mathbf{k}'-\mathbf{k})\mathbf{R}_i}\, \eta_{\mathbf{k}} V_{\mathbf{k}'}\, c^\dagger_{\mathbf{k}\sigma} c_{\mathbf{k}'\sigma'} \hat{f}^\dagger_{i\sigma'} \hat{f}_{i\sigma} + \mathrm{h.c.} \\ &- \frac{1}{N} \sum_{\mathbf{k}\sigma} \sum_{ij} 2 e^{-i\mathbf{k}(\mathbf{R}_i - \mathbf{R}_j)} \eta_{\mathbf{k}} V_{\mathbf{k}}\, \hat{f}^\dagger_{i\sigma} \hat{f}_{j\sigma}. \end{aligned} \quad (14)$$

In the first term we recognise a contribution, which possesses the form of the hybridisation interaction. The last term represents the generated hopping of the correlated f electrons, whose generation we have already discussed in the last paragraph. In terms of Hubbard operators both contributions can be characterised as one-particle contributions, whereas the remaining part is comprised of two-particle interactions. The second and the third term both correspond to a hybridisation-like interaction, which couples to an empty and a singly occupied f site, respectively. Alike the usual hybridisation term they alter the number of particles in the respective electron subsystem by one. In contrast the interactions in the fourth and fifth line do not change the number of particles within the conduction band or within the f electron subsystem. The penultimate term can be regarded a Coqblin-Schrieffer interaction.

To cope with all contributions of equation (14) we are obliged to introduce a truncation scheme. The objective of this is to keep the Hamiltonian in the form (13). This task may be accomplished by various techniques, one of them is the normal ordering of the operators [4]. Because normal ordering must be defined with respect to a bilinear Hamiltonian, it is more convenient to use an alternative scheme here. We simply decouple the higher interactions by use of a Hartree-Fock decoupling. In this context the fourth line of (14) is evaluated as

$$\begin{aligned}&\frac{1}{N} \sum_{\mathbf{k}\mathbf{k}'} \sum_{i\sigma} e^{i(\mathbf{k}'-\mathbf{k})\mathbf{R}_i}\, \eta_{\mathbf{k}} V_{\mathbf{k}'}\, c^\dagger_{\mathbf{k}\sigma} c_{\mathbf{k}'\sigma} P^0_i + \mathrm{h.c.} \\ &\to\ 2 \sum_{\mathbf{k}\sigma} \eta_{\mathbf{k}} V_{\mathbf{k}} \langle P^0_i \rangle\, c^\dagger_{\mathbf{k}\sigma} c_{\mathbf{k}\sigma} - \frac{2}{N} \sum_{i\mathbf{k}} \sum_{\sigma\sigma'} \eta_{\mathbf{k}} V_{\mathbf{k}} \langle n^c_{\mathbf{k}\sigma} \rangle\, \hat{f}^\dagger_{i\sigma'} \hat{f}_{i\sigma'} \\ &+ \frac{2}{N} \sum_{i\mathbf{k}\sigma} \eta_{\mathbf{k}} V_{\mathbf{k}} \langle n^c_{\mathbf{k}\sigma} \rangle \big(1 - \langle P^0_i \rangle\big) \end{aligned} \quad (15)$$

where the representation $\langle n^c_{\mathbf{k}\sigma} \rangle = \langle c^\dagger_{\mathbf{k}\sigma} c_{\mathbf{k}\sigma} \rangle$ and the relation $P^0_i + \sum_\sigma \hat{f}^\dagger_{i\sigma} \hat{f}_{i\sigma} = \mathbf{1}$ were used. Here the expectation values are to be evaluated with regard to the Hamiltonian (1), thus they are constant during the entire flow. Obviously, the first two terms on the right hand side contribute to the one-particle terms of the Hamiltonian, whereas the last one results in an energy shift. It should be emphasised that this factorisation scheme preserves the character of the initial interaction with regard to the number of particles in each electron subsystem. In equation (15), for example, both the interaction on the left hand side and the resulting terms on the right hand side preserve the number of c and f electrons. Furthermore, the local projector P^0_i remains untouched by such a kind of approximation. A detailed derivation of the decoupling of the remaining interaction is given in Appendix A.

If we collect all the terms that are provided by the factorisation scheme, we recognise that the occurrence of the expectation value $\langle P^0_i \rangle$ is always accompanied by the expectation value $\langle n^f_{i\sigma} \rangle$. As we have mentioned above the first denotes the average number of empty f sites, and the latter represents the number of singly occupied f sites. Since we consider the non-magnetic phase in the present paper, we can deduce the relation $\langle n^f_{i\sigma} \rangle = (1 - \langle P^0_i \rangle)/\nu_f$ from the completeness relation for the local f configuration space. As a consequence of this we conclude that $\langle P^0_i \rangle$ is of order ν_f^0 whereas $\langle n^f_{i\sigma} \rangle$ is of order ν_f^{-1}. The same becomes obvious for the contributions for the energy ε_f, where the terms of order ν_f^0 come from the parts $\propto P^0_i$, and the terms of order ν_f^{-1} are given by the contributions $\propto \hat{f}^\dagger_{i\sigma} \hat{f}_{i\sigma}$. As a simplification we consider in the following the case of great degeneracy of the electrons, i.e. $\nu_f \to \infty$, and neglect all terms of order ν_f^{-1}. The spirit of this approximation is rather similar to the SBMF theory, though both approaches cannot be simply compared on this level. Eventually, we arrive at the following system of differential equations for the one-particle energies of the

Hamiltonian (13)

$$\frac{\mathrm{d}\varepsilon_{\mathbf{k}}}{\mathrm{d}\ell} = 2\langle P_i^0\rangle \eta_{\mathbf{k}} V_{\mathbf{k}} \tag{16}$$

$$\frac{\mathrm{d}\Delta_{\mathbf{k}}}{\mathrm{d}\ell} = -2\eta_{\mathbf{k}} V_{\mathbf{k}} \tag{17}$$

$$\frac{\mathrm{d}\varepsilon_f}{\mathrm{d}\ell} = -\frac{2}{N}\sum_{\mathbf{k}\sigma}\langle n^c_{\mathbf{k}\sigma}\rangle \eta_{\mathbf{k}} V_{\mathbf{k}} - \frac{1}{N}\sum_{\mathbf{k}\sigma}\langle A_{\mathbf{k}\sigma}\rangle \eta_{\mathbf{k}}\Delta_{\mathbf{k}} \tag{18}$$

$$\frac{\mathrm{d}V_{\mathbf{k}}}{\mathrm{d}\ell} = -\big(\varepsilon_{\mathbf{k}} - \varepsilon_f - \langle P_i^0\rangle\Delta_{\mathbf{k}}\big)\eta_{\mathbf{k}} \tag{19}$$

$$\frac{\mathrm{d}E}{\mathrm{d}\ell} = \frac{2}{N}\sum_{i\mathbf{k}\sigma}\langle n^c_{\mathbf{k}\sigma}\rangle\big(1-\langle P_i^0\rangle\big)\eta_{\mathbf{k}} V_{\mathbf{k}} + \frac{1}{N}\sum_{i\mathbf{k}\sigma}\langle A_{\mathbf{k}\sigma}\rangle\big(1-\langle P_i^0\rangle\big)\eta_{\mathbf{k}}\Delta_{\mathbf{k}}. \tag{20}$$

The system possesses the initial conditions $\varepsilon_{\mathbf{k}}(\ell=0) = \varepsilon^{\mathrm{i}}_{\mathbf{k}}$, $\varepsilon_f(\ell=0) = \varepsilon^{\mathrm{i}}_f$, $V_{\mathbf{k}}(\ell=0) = V^{\mathrm{i}}_{\mathbf{k}}$ and $\Delta_{\mathbf{k}}(\ell=0) = E(\ell=0) = 0$. From the above equations we can immediately conclude $\langle P_i^0\rangle\Delta_{\mathbf{k}}(\ell) = \varepsilon^{\mathrm{i}}_{\mathbf{k}} - \varepsilon_{\mathbf{k}}(\ell)$ and $E(\ell) = N(\varepsilon^{\mathrm{i}}_f - \varepsilon_f(\ell))(1-\langle P_i^0\rangle)$ so that $\Delta_{\mathbf{k}}$ can be eliminated completely, by making use of the first relation.

At this point we emphasise that we have not used perturbational arguments with respect to the hybridisation strength nor have we used a mean-field decoupling of the Coulomb interaction within the above approximation scheme. This fact is very important with regard to the description of heavy fermion behaviour.

With the form-invariant Hamiltonian (13) we know that in the limit $\ell \to \infty$ the resulting effective Hamiltonian is of the form

$$H^*_{\mathrm{PAM}} = \sum_{\mathbf{k}\sigma}\varepsilon^*_{\mathbf{k}} c^\dagger_{\mathbf{k}\sigma} c_{\mathbf{k}\sigma} + \sum_{\mathbf{k}\sigma}\big(\varepsilon^*_f + \Delta^*_{\mathbf{k}}\big)\hat{f}^\dagger_{\mathbf{k}\sigma}\hat{f}_{\mathbf{k}\sigma} + E^*. \tag{21}$$

It describes two decoupled subsystems of uncorrelated and correlated electrons and can therefore not be regarded as diagonal. This fact is the main difference to other approaches, such as the SBMF theory, which leave a non-interacting Hamiltonian. Another important difference is that we do not need to incorporate a side condition, which restricts the number of particles on each f sites, for we did not made use of auxiliary boson fields.

3.2 Flow of observables

In the introduction we have already discussed the representation of expectation values within the framework of flow equations. There we concluded that expectation values as well as correlation functions can be easily evaluated on the basis of the derived effective Hamiltonian, if we regard the transformed operators at the same time. The transformation of an arbitrary operator works quite similar to the transformation of the Hamiltonian. If we consider, in the first instance, the flow of the operator $c_{\mathbf{k}\sigma}$, we can write the mapping in the form

$$\frac{\mathrm{d}c_{\mathbf{k}\sigma}}{\mathrm{d}\ell} = \big[\eta, c_{\mathbf{k}\sigma}\big]. \tag{22}$$

Similar to the transformation of the Hamiltonian we have to regard all the contributions that are generated by the commutator on the right hand side. The operator, of course, has to fulfil the boundary condition $c_{\mathbf{k}\sigma}(0) = c_{\mathbf{k}\sigma}$. Hence we obtain the lowest order contributions simply by evaluating the commutator with $c_{\mathbf{k}\sigma}$. With this results we can infer the following form for the ℓ-dependent operator

$$c_{\mathbf{k}\sigma}(\ell) = \alpha_{\mathbf{k}}\, c_{\mathbf{k}\sigma} + \beta_{\mathbf{k}}\, \hat{f}_{\mathbf{k}\sigma}. \tag{23}$$

This is a linear combination of the ordinary operators $c_{\mathbf{k}\sigma}$ and $\hat{f}_{\mathbf{k}\sigma}$ with the weighting factors $\alpha_{\mathbf{k}}$ and $\beta_{\mathbf{k}}$, respectively. It is the simplest possible representation for the flow of the operator $c_{\mathbf{k}\sigma}$, and higher interactions that are generated by the commutator must be truncated in the same manner as we have treated the flow of the Hamiltonian [23]. The complete evaluation of the flow equation (22) yields differential equations for the weighting factors

$$\frac{\mathrm{d}\alpha_{\mathbf{k}}}{\mathrm{d}\ell} = -\beta_{\mathbf{k}}\eta_{\mathbf{k}}\langle P_i^0\rangle\ , \quad \frac{\mathrm{d}\beta_{\mathbf{k}}}{\mathrm{d}\ell} = \alpha_{\mathbf{k}}\eta_{\mathbf{k}}. \tag{24}$$

Here again the ℓ-dependence has been omitted for the reason of readability. Obviously, the initial values of the weight factors are given by $\alpha^{\mathrm{i}}_{\mathbf{k}} = 1$ and $\beta^{\mathrm{i}}_{\mathbf{k}} = 0$, and as a consequence of unitarity they obey the relation

$$\alpha^2_{\mathbf{k}} + \langle P_i^0\rangle\beta^2_{\mathbf{k}} = 1. \tag{25}$$

In a further step the coefficient $\beta_{\mathbf{k}}$ can be eliminated, and the flow of $\alpha_{\mathbf{k}}$ is governed by the equation

$$\frac{\mathrm{d}}{\mathrm{d}\ell}\arcsin\big[1-2\alpha^2_{\mathbf{k}}\big] = 2\sqrt{\langle P_i^0\rangle}\eta_{\mathbf{k}}. \tag{26}$$

The transformation of the operator $\hat{f}_{\mathbf{k}\sigma}$ can be treated likewise, and we obtain

$$\hat{f}_{\mathbf{k}\sigma}(\ell) = -\langle P_i^0\rangle\beta_{\mathbf{k}}\, c_{\mathbf{k}\sigma} + \alpha_{\mathbf{k}}\, \hat{f}_{\mathbf{k}\sigma}. \tag{27}$$

With the results of the previous paragraph we are now in the position to evaluate all expectation values that occur in the differential equations by using the unitarity of the transformation, i.e. $\langle n_{\mathbf{k}\sigma}\rangle = {}^*\langle c^{*\dagger}_{\mathbf{k}\sigma} c^*_{\mathbf{k}\sigma}\rangle^*$. Here ${}^*\langle\cdots\rangle^*$ refers to the expectation value with respect to the fully transformed Hamiltonian (21). By inserting the transformed operators, we obtain for the non-local expectation values

$$\langle n_{\mathbf{k}\sigma}\rangle = (\alpha^*_{\mathbf{k}})^2\, {}^*\langle c^\dagger_{\mathbf{k}\sigma} c_{\mathbf{k}\sigma}\rangle^* + (\beta^*_{\mathbf{k}})^2\, {}^*\langle \hat{f}^\dagger_{\mathbf{k}\sigma}\hat{f}_{\mathbf{k}\sigma}\rangle^* \tag{28}$$

and

$$\langle A_{\mathbf{k}\sigma}\rangle = 2\,\alpha^*_{\mathbf{k}}\beta^*_{\mathbf{k}}\left(-\langle P_i^0\rangle^*\langle c^\dagger_{\mathbf{k}\sigma} c_{\mathbf{k}\sigma}\rangle^* + {}^*\langle \hat{f}^\dagger_{\mathbf{k}\sigma}\hat{f}_{\mathbf{k}\sigma}\rangle^*\right). \tag{29}$$

In view of the Hamiltonian (21) it is clear that there are no contributions from expectation values of the form ${}^*\langle c^\dagger_{\mathbf{k}\sigma}\hat{f}_{\mathbf{k}\sigma}\rangle^*$.

The derivation of the non-local expectation values, which contain contributions from different lattice sites, could be carried out rather intuitively, since we made use

of a descriptive transformation scheme for the single operators. In contrast, the treatment of the local expectation value $\langle P_i^0 \rangle$ turns out to be more difficult. Though the projector can be represented in terms of Hubbard operators as $P_i^0 = \hat{f}_{i\sigma}^\dagger \hat{f}_{i\sigma}$, its transformation cannot simply be carried out by the transformation of the single operators, for this procedure would break the restriction for the f electrons to empty and singly occupied sites. Instead of that we must transform the entire operator P_i^0. The detailed derivation of this expectation value is presented in Appendix B, and as result we obtain

$$\langle P_i^0 \rangle = 1 - \frac{1}{N} \sum_{\mathbf{k}\sigma} \Big[\big(1 - (\alpha_{\mathbf{k}}^*)^2\big) \, {}^*\langle c_{\mathbf{k}\sigma}^\dagger c_{\mathbf{k}\sigma} \rangle^* + \big(1 - (\beta_{\mathbf{k}}^*)^2\big) \, {}^*\langle \hat{f}_{\mathbf{k}\sigma}^\dagger \hat{f}_{\mathbf{k}\sigma} \rangle^* \Big]. \quad (30)$$

Altogether, this more sophisticated treatment can also be applied in order to derive the non-local expectation values, if we transform them as pairs rather than as single operators. The result of this evaluation, though, coincides with the above derivation, and we can use the much easier representation from the last paragraph first for reasons of clearness and second as a starting point for the evaluation of the Green's functions.

Further on, we wish to discuss the form of the expectation value which is provided by (30). If we alternatively start out from the fact that the total number of particles must be conserved under the unitary transformation, we can derive this result in another way. The relation

$$\sum_{\mathbf{k}\sigma} \langle n_{\mathbf{k}\sigma}^c \rangle + \sum_{i\sigma} \langle \hat{f}_{i\sigma}^\dagger \hat{f}_{i\sigma} \rangle = \sum_{\mathbf{k}\sigma} {}^*\langle c_{\mathbf{k}\sigma}^\dagger c_{\mathbf{k}\sigma} \rangle^* + \sum_{\mathbf{k}\sigma} {}^*\langle \hat{f}_{\mathbf{k}\sigma}^\dagger \hat{f}_{\mathbf{k}\sigma} \rangle^* \quad (31)$$

denotes the particle number conservation. If we use on the left hand side the expression (28) for the expectation value $\langle n_{\mathbf{k}\sigma}^c \rangle$ and divide by the number of sites, we eventually arrive at equation (30). Consequently, we can deduce that the above derivation is consistent with the conservation of the total number of particles.

As a remaining task we have to evaluate the expectation values ${}^*\langle c_{\mathbf{k}\sigma}^\dagger c_{\mathbf{k}\sigma} \rangle^*$ and ${}^*\langle \hat{f}_{\mathbf{k}\sigma}^\dagger \hat{f}_{\mathbf{k}\sigma} \rangle^*$ with respect to the effective Hamiltonian (21). As the subsystem of c electrons simply consists of non-interacting fermions the respective expression is determined by a Fermi distribution. The calculation of the remaining f-subsystem is more complex as these particles do not obey a simple statistics. It is expedient to calculate the demanded expectation value by means of ordinary Green's function calculations [24]. The equation of motion for the f Green's function is simply given by

$$\omega \, \langle\langle \hat{f}_{\mathbf{k}\sigma}; \hat{f}_{\mathbf{k}\sigma}^\dagger \rangle\rangle(\omega + i\delta) = \big\langle \big\{ \hat{f}_{\mathbf{k}\sigma}, \hat{f}_{\mathbf{k}\sigma}^\dagger \big\}_+ \big\rangle + \big\langle \big\langle \big[\hat{f}_{\mathbf{k}\sigma}, H^* \big]; \hat{f}_{\mathbf{k}\sigma}^\dagger \big\rangle \big\rangle(\omega + i\delta) \quad (32)$$

where we set $\hbar = 1$. This representation suggests a coupling to higher order Green's functions, which can be seen by the second term on the right hand side. In order to obtain a closed equation of motion we again apply the decoupling scheme of the last section and neglect contributions of order ν_f^{-1}. As result we obtain

$$\langle\langle \hat{f}_{\mathbf{k}\sigma}; \hat{f}_{\mathbf{k}\sigma}^\dagger \rangle\rangle(\omega + i\delta) = \frac{\langle P_i^0 \rangle}{\omega + is - (\varepsilon_f^* + \langle P_i^0 \rangle \Delta_{\mathbf{k}}^*)} \quad (33)$$

and, by the application of the spectral theorem, the desired expectation value reads

$${}^*\langle \hat{f}_{\mathbf{k}\sigma}^\dagger \hat{f}_{\mathbf{k}\sigma} \rangle^* = \langle P_i^0 \rangle \, n_{\mathrm{F}}\big(\varepsilon_f^* + \langle P_i^0 \rangle \Delta_{\mathbf{k}}^*\big). \quad (34)$$

On the right hand side the Fermi distribution $n_{\mathrm{F}} = (1 + \exp(\beta E))^{-1}$ has been introduced.

4 Integration of the flow equations

4.1 Analytical solution

The PAM during the flow is given by equation (13) and leads to an effective Hamiltonian of the form (21), provided we have chosen a generator which ensures the vanishing of the hybridisation $V_{\mathbf{k}}$. The evolution of the matrix elements is given by a closed set of coupled differential equations, which have to be evaluated for the derivation of physical quantities. In a first step we try to find an analytical solution. For this purpose we bring equation (19) in the following form

$$\eta_{\mathbf{k}} = -\frac{1}{2\varepsilon_{\mathbf{k}} - \varepsilon_f - \varepsilon_{\mathbf{k}}^{\mathrm{i}}} \frac{\mathrm{d}V_{\mathbf{k}}}{\mathrm{d}\ell}. \quad (35)$$

Here we have substituted $\Delta_{\mathbf{k}}$ following the above discussion. This equation provides a representation of $\eta_{\mathbf{k}}$ as function of the one-particle energies and allows us to eliminate this quantity in all other differential equations. With equation (35) we are now in the position to rewrite the differential equation for the single-particle energy $\varepsilon_{\mathbf{k}}$ as

$$\frac{\mathrm{d}}{\mathrm{d}\ell} \big[\varepsilon_{\mathbf{k}}^2 - \varepsilon_{\mathbf{k}} (\varepsilon_f^* + \varepsilon_{\mathbf{k}}^{\mathrm{i}}) + \langle P_i^0 \rangle V_{\mathbf{k}}^2 \big] = (\varepsilon_f - \varepsilon_f^*) \frac{\mathrm{d}\varepsilon_{\mathbf{k}}}{\mathrm{d}\ell}. \quad (36)$$

As a simplification for the next discussions we assume that the energy ε_f converges rather fast to its limit value, while the main contribution to the evolution of the other energies occur at a larger ℓ-scale. This assumption allows us to replace $\varepsilon_f(\ell)$ by the constant energy ε_f^*. Such kind of simplification is quite common in terms of flow equations [21,22]. With this approximation the equation (36) can simply be integrated and we arrive at

$$(\varepsilon_{\mathbf{k}}^*)^2 - \varepsilon_{\mathbf{k}}^* \big(\varepsilon_f^* + \varepsilon_{\mathbf{k}}^{\mathrm{i}}\big) + \varepsilon_{\mathbf{k}}^{\mathrm{i}} \varepsilon_f^* - \langle P_i^0 \rangle (V_{\mathbf{k}}^{\mathrm{i}})^2 = 0 \quad (37)$$

using the fact that $V_{\mathbf{k}}$ vanishes in the limit $\ell \to \infty$. This quadratic equation has the solutions

$$\varepsilon_{\mathbf{k}}^* = \frac{1}{2}\big(\varepsilon_f^* + \varepsilon_{\mathbf{k}}^{\mathrm{i}}\big) \pm \frac{1}{2} W_{\mathbf{k}} \quad (38)$$

where we have used the representation

$$W_{\mathbf{k}} = \sqrt{\big(\varepsilon_f^* - \varepsilon_{\mathbf{k}}^{\mathrm{i}}\big)^2 + 4 \langle P_i^0 \rangle (V_{\mathbf{k}}^{\mathrm{i}})^2}. \quad (39)$$

Equivalently, we obtain the following solution for the f degrees of freedom

$$\varepsilon_f^* + \langle P_i^0 \rangle \Delta_{\mathbf{k}}^* = \frac{1}{2}\left(\varepsilon_f^* + \varepsilon_{\mathbf{k}}^{\mathrm{i}}\right) \mp \frac{1}{2} W_{\mathbf{k}}. \tag{40}$$

The latter describes the excitation energies of the f electrons as suggested by equation (34). In order to derive a simple equation for the energy ε_f we neglect the term with $\langle A_{\mathbf{k}\sigma} \rangle$ on the right hand side of (18), and after having integrated the resulting equation, we obtain

$$\varepsilon_f^* - \varepsilon_f^{\mathrm{i}} = -\frac{1}{N} \sum_{\mathbf{k}\sigma} \frac{\langle n_{\mathbf{k}\sigma}^c \rangle}{\langle P_i^0 \rangle} (\varepsilon_{\mathbf{k}}^* - \varepsilon_{\mathbf{k}}^{\mathrm{i}}) = -\frac{1}{N} \sum_{\mathbf{k}\sigma} \frac{\langle n_{\mathbf{k}\sigma}^c \rangle (V_{\mathbf{k}}^{\mathrm{i}})^2}{\varepsilon_f^* - \varepsilon_{\mathbf{k}}^*}. \tag{41}$$

The simplification of a constant energy ε_f can also be made for the derivation of the weighting factors and allow us the evaluation of expectation values. From (26) we arrive at

$$(\alpha_{\mathbf{k}}^*)^2 = \frac{1}{2}\left(1 + \frac{\varepsilon_f^* - \varepsilon_{\mathbf{k}}^{\mathrm{i}}}{W_{\mathbf{k}}}\right). \tag{42}$$

Altogether the results coincide with the expressions from the SBMF theory. The excitation energies (38) and (40) constitute the electronic structure of the system of two gapped bands. The overall renormalisation of the f level is provided by equation (41). These results are based on the assumption of a fast convergence of ε_f compared to all other energies and give us a rough estimate of the electronic structure of the full problem. However, a thorough examination beyond this simplification requires a numerical treatment of the differential equations. We would like to stress that we have not used a particular choice for the coefficient $\eta_{\mathbf{k}}$. Thus the derived results are valid for any $\eta_{\mathbf{k}}$ that yields a vanishing hybridisation for the fully transformed Hamiltonian.

4.2 Numerical solution

The above derivation of an analytical solution for the differential equations was based on further simplifications. A more general solution can be provided by a numerical integration. While the analytical solution was independent of a particular choice of the coefficient $\eta_{\mathbf{k}}$, we now need to determine this quantity for the numerical evaluation. An expedient choice is given by

$$\eta_{\mathbf{k}} = \left(2\varepsilon_{\mathbf{k}} - \varepsilon_f - \varepsilon_{\mathbf{k}}^{\mathrm{i}}\right) V_{\mathbf{k}} \tag{43}$$

since the energy $V_{\mathbf{k}}$ vanishes when ℓ goes to infinity. This becomes obvious by inserting equation (43) into equation (19), for the differential of $V_{\mathbf{k}}$ is a negative quantity in the entire integration range, while $V_{\mathbf{k}}$ itself is always positive. The above choice is not dissimilar to Wegner's generator. However, it is not simply obtained by commuting the interacting and the non-interacting part of the Hamiltonian, as suggested by equation (7), in that the non-interacting part for the present calculations incorporates the hopping of strongly correlated objects. In fact, the derivation of the generator (43) uses a factorisation scheme, which has been presented in detail in Section 3.1. This particular form of the generator also triggers the Hamiltonian flowing into a stable fixed point, as η commutes with H_{PAM} in the limit $\ell \to \infty$. As a consequence the differentials of the one-particle energies vanish in this limit, which can be seen on the basis of equations (16–20).

The numerics generally comprises two tasks, one of them being the numerical integration of the flow equations, which is done by a Runge-Kutta integration of fifth order with adaptive step size control. The second part of the numerical calculation is the self-consistent evaluation of the expectation values $\langle P_i^0 \rangle$, $\langle n_{\mathbf{k}\sigma}^c \rangle$ and $\langle A_{\mathbf{k}\sigma} \rangle$.

Since the differential equations are coupled and possess a dependence on $\mathbf{k}$-dependent expectation values, the numerical integration turns out to be a rather arduous task. Consequently, we restrict ourselves to the solution of a one-dimensional system. As we consider merely the paramagnetic phase of the PAM, we believe that one dimension is sufficient to examine the most general aspects of heavy-fermion behaviour.

5 Results

In the following section we present the results of the numerical calculations for the PAM. In a first step we analyse the flow of the one-particle energies of the Hamiltonian. All calculations are performed for systems of 1000 sites in one dimension. As we have mentioned above, we merely consider a dispersion-less hybridisation. Notwithstanding, the hybridisation $V_{\mathbf{k}}$ shows distinct flows for different wave vectors $\mathbf{k}$ due to its dependence on the electron energies (cf. Eq. (19)). For the conduction electrons we use a constant density of states (DOS), i.e. a linear dispersion in one dimension, and we consider $T = 0$.

For the upcoming discussions we use lattice constant of $a = 1$ and $W = 2$ for the bandwidth of the bare conduction band, so that all energies are given in units of the half band width, which is usually of order $1 - 10$ eV $\sim 10^4 - 10^5$ K. As we consider one-dimensional systems, the wave vector is rather referred to as wave number.

5.1 One-particle energies

In the following discussion we address the one-particle energies $\varepsilon_{\mathbf{k}}$, ε_f and $V_{\mathbf{k}}$. For a particular parameter regime their flow diagrams are depicted in Figures 1 and 2. For the electron energies it is more convenient to investigate the difference to their initial value, namely $\varepsilon_{\mathbf{k}}(\ell) - \varepsilon_{\mathbf{k}}^{\mathrm{i}}$, as a function of the flow parameter ℓ. This quantity is shown in Figure 1 for a range of wave numbers near the crossing point. The latter is characterised as the particular wave number, that divides the energies between increasing and decreasing quantities. This behaviour can be understood on the basis of equation (16), as the sign of the right hand side depends on the wave number. For the system in Figure 1 we find positive energy differences $\varepsilon_{\mathbf{k}}^* - \varepsilon_{\mathbf{k}}^{\mathrm{i}}$ above a critical wave number of $\mathbf{k} = 0.499\pi$. As the graph shows,

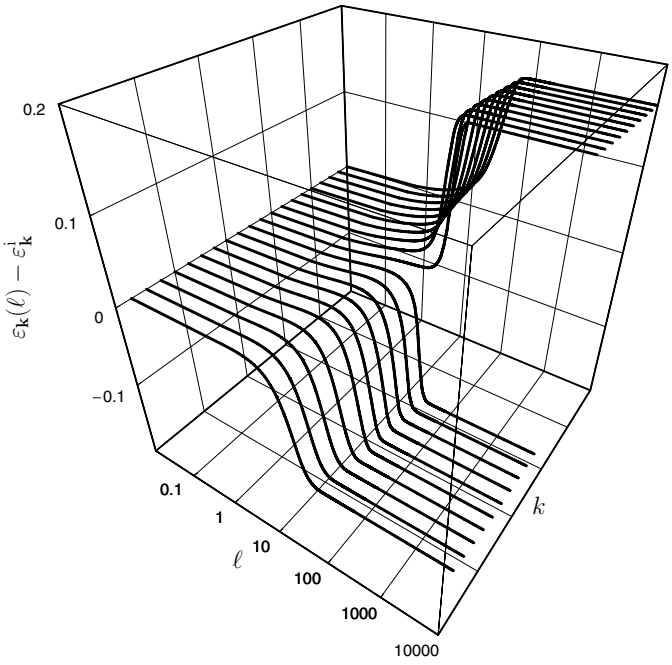

Fig. 1. Flow of the quantities $\varepsilon_{\mathbf{k}} - \varepsilon^{\mathrm{i}}_{\mathbf{k}}$ for subset wave numbers near the critical wave number (see text) for a system with $\varepsilon^{\mathrm{i}}_f = 0.9$, $V^{\mathrm{i}} = 0.3$ and $\nu_f = 2$.

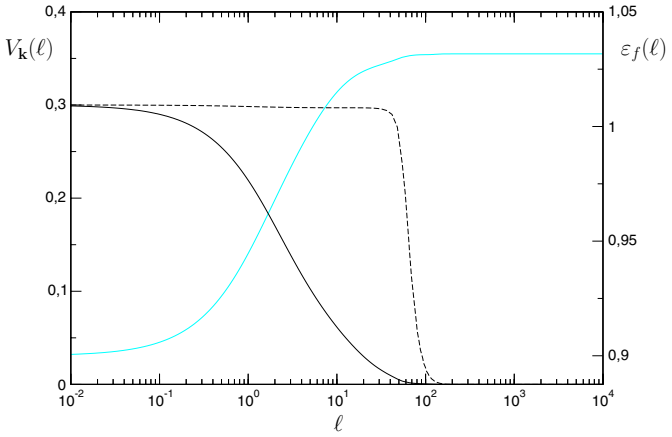

Fig. 2. Flow of the quantities $V = 1/N \sum_{\mathbf{k}} V_{\mathbf{k}}$ (black solid line, left scale), $V_{\mathbf{k}}$ for the critical wave number (black dashed line, left scale) and ε_f (blue solid line, right scale). The system parameters are as in Figure 1.

all energies start off with small modifications up to values of $\ell \simeq 1$ before they enter a region of significant rise or fall. In the region of $\ell \gtrsim 10^2$ they have already converged to their limit value. The most remarkable result of their behaviour is definitely the sharp crossover between increasing and decreasing energies.

A much simpler picture is provided by the graphs in Figure 2. As demanded, the hybridisation energy $V_{\mathbf{k}}$ vanishes for all wave vectors for $\ell \gtrsim 10^2$. In Figure 2 the flow of the quantity $V = 1/N \sum_{\mathbf{k}} V_{\mathbf{k}}$ is shown (solid black line) beside the flow of the hybridisation $V_{\mathbf{k}}$ for the critical wave number $\mathbf{k} = 0.499\pi$. For the latter the onset of a significant modification is delayed to higher values of ℓ, and it drops sharply to zero in the region of $\ell \simeq 10^2$. This suggests that the $V_{\mathbf{k}}$ with wave numbers near the upper and lower band edge are renormalised at lower values of ℓ. Altogether we can conclude that all hybridisation elements can be considered zero above $\ell \simeq 10^2$. On the other hand the one-particle energy which characterises the local f level sees a sharp increase in the region of $\ell \sim 10^0 - 10^1$ and converges rather fast. The numerical results show that the present choice for $\eta_{\mathbf{k}}$ triggers a smooth and continuous evolution of the one-particle energies of the Hamiltonian (13). The convergence to their limit values occurs on a characteristic scale in the region of $\ell \gtrsim 10^2$. For the present results we use the bound $V = 10^{-10}$ as convergence criteria for the numerical integration of the flow equations. This corresponds to a value of the flow parameter $\ell \sim 3000 - 5000$ in the considered parameter regimes. However, for a better clearness the integration for the system in Figure 2 is carried out up to a value of $\ell = 10^4$.

On the one hand we have a rather good convergence of the flow equations due to their smoothness and their evolution to a stable fixed point. On the other hand the self-consistent evaluation of the expectation values is restricted to certain parameter regimes. From the SBMF theory we know that it cannot describe the phase where all f sites are singly occupied, i.e. $\langle P^0_i \rangle = 0$. Likewise, in the present approach we only obtain valid results for a finite number of empty f sites, and the solution breaks down as $\langle P^0_i \rangle$ vanishes. This breakdown coincides with the energy ε^*_f dropping below the chemical potential. However, it is possible to obtain solutions near this critical point. The limit of singly occupied f sites can be approached either by decreasing the hybridisation energy or by increasing the difference $\mu - \varepsilon^{\mathrm{i}}_f$. With a fixed value for $\varepsilon^{\mathrm{i}}_f$ the solution breaks down below a critical value of V^{i}, and, similarly, this point is reached for a fixed V^{i} below a critical $\varepsilon^{\mathrm{i}}_f$. Stable solutions for small expectation values $\langle P^0_i \rangle$ can be obtained, preferably, at rather moderate values of $\mu - \varepsilon^{\mathrm{i}}_f$ and small V^{i}. This restriction is believed to be lifted up by considering corrections of order ν_f^{-1} [25].

Within the above factorisation scheme it is not sufficient to incorporate the ν_f^{-1} contributions simply by considering them in equations (16–20). Indeed, it turns out that this procedure would lead to unphysical solutions especially in the case of small ν_f. On the other hand the dynamics of the f electrons is even more affected by these corrections and cannot be properly calculated in the limit of small degeneracy. A consistent consideration of the ν_f therefore needs an enhancement of the factorisation process. As we pointed out in Section 3.1 the decoupling of the higher order interactions preserves their character with respect to the variation of the particle numbers for each subsystem. This assumption is too restrictive in the case of small degeneracy, as charge fluctuations which are induced by the flow of the Hamiltonian become more important. Obviously, the extension of the factorisation scheme in this sense would lead to a more complex system of differential equations and is not considered in the present work.

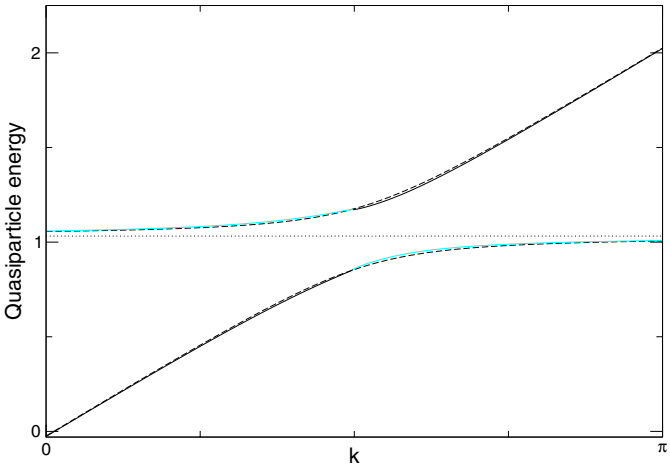

Fig. 3. Dispersion of the quasiparticles for the system with parameters as in Figure 1. The energies $\varepsilon^*_{\mathbf{k}}$ and $\varepsilon^*_f + \langle P^0_i \rangle \Delta^*_{\mathbf{k}}$ are represented by solid black and blue lines, respectively, whereas the the analytical dispersions are represented by staggered lines. The dotted line stands for ε^*_f.

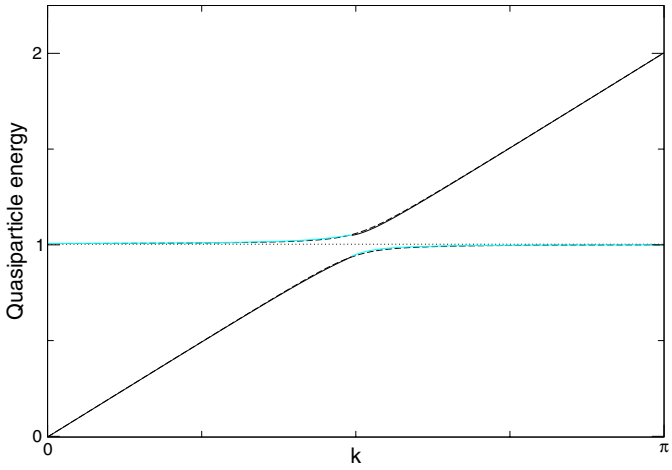

Fig. 4. Dispersion of the quasiparticles as in Figure 3 for a system with $\varepsilon^{\mathrm{i}}_f = 0.9$, $V^{\mathrm{i}} = 0.2$ and $\nu_f = 2$.

5.2 Electronic properties

In this section we present the numerical results for the electronic structure of the PAM. The dispersion relations of the quasiparticle energies are shown in Figures 3 and 4. The general form of the one-particle energies is quite similar to the results of the SBMF theory. In both approaches the spectrum splits in two bands which are divided by a finite gap. Considering the chemical potential lying in one of the bands, the system possesses a metallic ground state. The situation of an insulator is also conceivable, if μ is right in the gap. In the following considerations we only focus on the metallic case, though the insulating case can also be examined within the framework of flow equations [26].

The quasiparticle energies in Figure 3 are obtained for a system with $\varepsilon^{\mathrm{i}}_f = 0.9$, $V^{\mathrm{i}} = 0.3$ and $\nu_f = 2$. The chemical potential is at $\mu = 1$ and the bandwidth of the conduction electron band is $W = 2$. Since we have neglected terms of order ν_f^{-1} within our calculations, the presented results for a twofold degenerate f level are deemed an extrapolation down to small values of ν_f. This kind of assumption has been frequently used in terms of various $1/\nu_f$ expansions in order to describe physical relevant systems. The excitation energies $\varepsilon^*_{\mathbf{k}}$ (solid black line) and $\varepsilon^*_f + \langle P^0_i \rangle$ (solid blue line) form two continuous bands, that are separated by an indirect gap. The latter denotation refers to the fact, that the minimal excitation energy from the lower to the upper band occurs at different wave vectors. The renormalised energy ε^*_f (dotted line) lies right in the centre of this gap. The self-consistently evaluated results for this energy and for the expectation value of the empty f sites are obtained as $\varepsilon^*_f = 1.032$ and $\langle P^0_i \rangle = 0.285$, which states, that the system is well within the mixed-valent regime. Though the results from the SBMF theory of $\varepsilon^*_{f,\mathrm{SB}} = 1.111$ and $\langle P^0_i \rangle_{\mathrm{SB}} = 0.577$ also suggest a mixed-valent system, the latter is significantly further away from the integral-valent state. This tendency is a general result of the flow equations approach and can be better understood in the context of a characteristic energy scale (cf. Sect. 5.3 below). The quasiparticle energies obtained from the numerical solution can be compared to those of the analytical treatment in Section 4.1. Their analytical expressions are given by equation (38) and equation (40), which have proved to be formally equivalent to the corresponding results of the SBMF theory. For the expectation value $\langle P^0_i \rangle$ and the energy ε^*_f we have used the numerically evaluated results in Figure 3. The graphs show a qualitatively good coincidence of both results for the excitation energies. However, near the crossing point of c-like and f-like excitations the deviations become most significant. Especially, the upper band shows a slight depletion near the crossing point, which results in a Van Hove-like singularity in the quasiparticle DOS. This feature is a result of the consideration of a renormalisation of the energy ε_f on a large ℓ-scale, which is driven by local fluctuations. The analytical solution is based on the assumption of a fast flow of this energy to its limit value, which is contrasted by Figures 1 and 2. Here we perceive the characteristic ℓ-scale of all energies in the same region. However, the quasiparticle energies of the analytical solution show a good correspondence to their numerical counterparts.

Whereas the system in Figure 3 was classified as mixed-valent system, Figure 4 is very close to the integral-valent or Kondo behaviour. This manifests itself in the very small expectation value $\langle P^0_i \rangle = 0.083$ and the energy $\varepsilon^*_f = 1.003$ lying only slightly above the chemical potential. This system also features an evident decrease of the gap width. In comparison with that result the SBMF theory delivers $\langle P^0_i \rangle_{\mathrm{SB}} = 0.479$ and $\varepsilon^*_{f,\mathrm{SB}} = 1.036$ indicating a mixed-valent behaviour. This distinctive tendency of the flow equation result towards integral-valence is discussed in connection with the Kondo temperature in Section 5.3 below.

The drastic change in the character of the quasiparticles from c to f character is a key result of the numerical calculations, as this contributions evolve from the bare

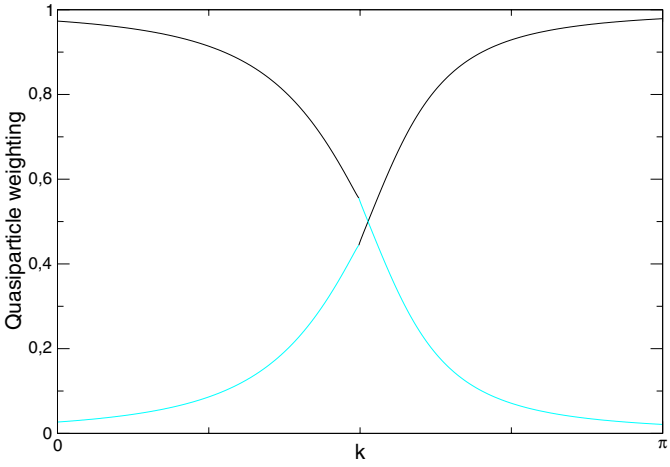

Fig. 5. Weighting factors $(\alpha^*_{\mathbf{k}})^2$ (black solid line) and $\langle P^0_i\rangle(\beta^*_{\mathbf{k}})^2$ for the same system as in Figure 3.

conduction electron band and the dispersion-less f level, respectively, during the flow. This fact also ensures the right result in the limit of a system without hybridisation. Notwithstanding, the different types of excitations form two continuous bands. In the context of the SBMF theory the side conditions are usually chosen in the way that each quasiparticle bands carries a single character. The switch of the excitation character in each band is also reflected by a change in the behaviour of the weighting factors $\alpha^*_{\mathbf{k}}$ and $\beta^*_{\mathbf{k}}$. The dispersion of their squares is shown in Figure 5. As the evaluation of the expectation values in Section 3.2 incorporates both the quasiparticle energies and the weighting factors, these quantities are not affected by the switch of the excitation character.

5.3 Kondo temperature

Historically, the Kondo temperature T_{K} was introduced as a low energy scale associated with the screening of a magnetic impurity in a metallic host. The microscopic models for the description of such a situation are the single impurity Anderson model (SIAM) and the single impurity Kondo model (KLM). Renormalisation group calculations [27] as well as SBMF theory [7,25] show a dependence of this energy scale on the Kondo coupling $J = (V^{\mathrm{i}})^2/|\varepsilon^{\mathrm{i}}_f - \mu|$ of the form

$$k_{\mathrm{B}}T_{\mathrm{K}} \propto \exp\left[-\frac{1}{J\nu_f\rho_0}\right]. \tag{44}$$

This relation states, that this energy scale vanishes exponentially as V^{i} goes to zero, a result that cannot be obtained by ordinary perturbation theory in V^{i}. In a periodic array of magnetic impurities beside the conventional screening of the local moments a coherence scale T^* seem to exist, which is referred to in the literature as coherence temperature, indicating the onset of Fermi-liquid behaviour. Whereas the Gutzwiller calculations for the PAM suggest a significant enhancement of T^* compared to the Kondo temperature of the SIAM, the SBMF theory provides a coincidence of both temperatures for small T^*. The comparison of both energy scales has been dedicated a controversial discussion. While some numerical works show an enhancement of T^* for systems at half filling [11], a more qualitative discussion by Nozières [28] relates this issue to the so-called exhaustion problem. As Nozières points out, only a fraction of $n_{\mathrm{scr}} = \rho_0 T_{\mathrm{K}}$ conduction electrons contributes to the screening of local moments. As a consequence of this, he deduces an upper bound of $T^* = \rho_0 T_{\mathrm{K}}^2/n_f$, where n_f is the number of magnetic impurities, for the lattice energy scale. This behaviour is supported by numerical calculations by Vidhyadhiraja et al. [13].

In accordance to the SBMF theory [25] we define the Kondo temperature by the difference of the renormalised f level and the chemical potential as

$$k_{\mathrm{B}}T^* = \varepsilon^*_f - \mu. \tag{45}$$

As we have mentioned at the beginning of this section, our method provides valid results in a certain parameter regime. By lowering the hybridisation V^{i} or by increasing the difference $\mu - \varepsilon^{\mathrm{i}}_f$ the self-consistency scheme breaks down as the expectation value $\langle P^0_i\rangle$ vanishes. The vanishing point coincides with $\varepsilon^{\mathrm{i}}_f$ slipping below the chemical potential, which is consistent with the assumption of positive results for the lattice Kondo temperature.

The evaluation of the Kondo temperature also allows us to estimate the resulting effective masses of the quasiparticles by comparing this energy scale to the band width of the bare conduction electrons. This leaves us with the relation $m^*/m \sim W/k_{\mathrm{B}}T^*$. If we consider the system in Figure 3, we obtain an effective quasiparticle mass of $m^*/m \sim 60$, indicating the system being in the mixed-valence regime. The enhancement of the quasiparticle mass is due to the flatness of the quasiparticle band near the Fermi surface, and it is also associated with a large quasiparticle DOS. For the integral-valence system in Figure 4 we even deduce an effective mass of $m^*/m \sim 600$.

To address the issue of the functional trend of the Kondo temperature for the numerical solution, we evaluate this quantity by varying the coupling J. In particular, we examine the dependence of T^* on the hybridisation V^{i}. The result for the system with $\varepsilon^{\mathrm{i}}_f = 0.9$ is shown in Figure 6. Here V^{i} is gradually decreased until the solution breaks down below the value $V^{\mathrm{i}} = 0.11$. The numerical results are represented by circles, and the blue solid line characterises the fit $\beta\exp(-\delta/J\nu_f\rho_0)$. Our findings for the fit parameters are $\beta = 0.20$ and $\delta = 1.65$. The latter identifies the value of the exponent and is significantly enhanced to the corresponding value for the SIAM, i.e. $\delta = 1$. That means that the lattice energy scale features a remarkable reduction. As we have mentioned above, this behaviour gives credence to the exhaustion scenario.

5.4 Green's functions

In Section 2.2 we have explained the evaluation of correlation functions within the framework of the flow equation

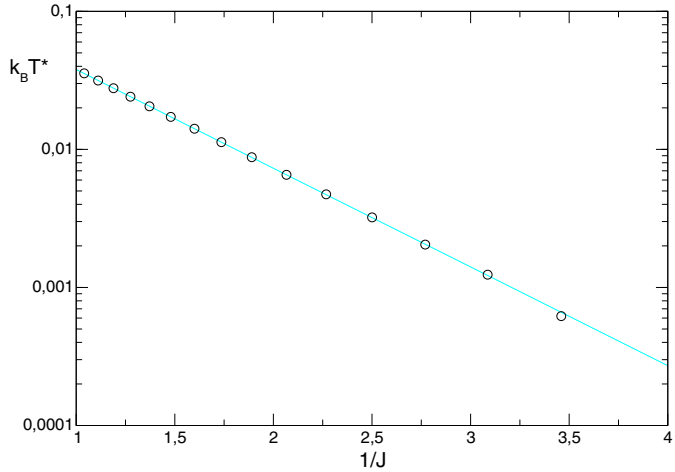

Fig. 6. Kondo temperature as a function of $1/J$ (see text) for a system with $\varepsilon_f^{\mathrm{i}} = 0.9$ and $\nu_f = 2$. The blue solid line represents the fit $\beta \exp(-\delta/J\nu_f\rho_0)$ with $\beta = 0.20$ and $\delta = 1.65$.

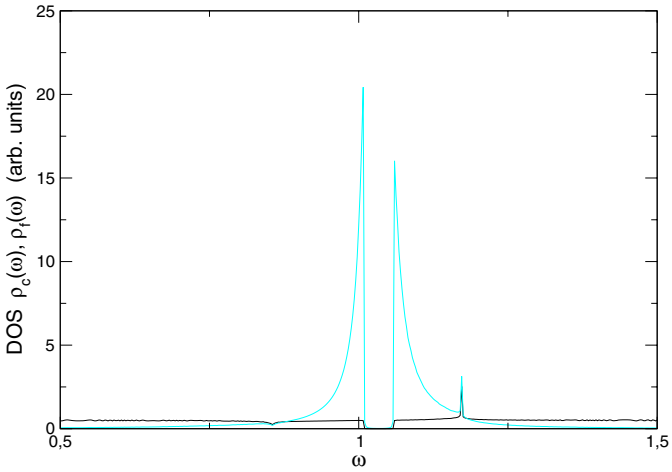

Fig. 7. Densities of state $\rho_c(\omega)$ (black solid line) and $\rho_f(\omega)$ (blue solid line) for the same system as in Figure 3.

method. As such quantities are invariant with respect to the unitary transformation, we are in the advantageous position of describing them with respect to a simple effective Hamiltonian. In this context we use the results for the transformed operators from Section 3.2. For the conduction electrons this yields

$$\langle\langle c_{\mathbf{k}\sigma}; c^\dagger_{\mathbf{k}\sigma}\rangle\rangle(\omega + i\delta) = \frac{(\alpha^*_{\mathbf{k}})^2}{\omega + i\delta - \varepsilon^*_{\mathbf{k}}} + \frac{\langle P^0_i\rangle(\beta^*_{\mathbf{k}})^2}{\omega + i\delta - (\varepsilon^*_f + \langle P^0_i\rangle \Delta^*_{\mathbf{k}})}. \quad (46)$$

Likewise we arrive at a representation for the f-electron Green's function:

$$\langle\langle \hat{f}_{\mathbf{k}\sigma}; \hat{f}^\dagger_{\mathbf{k}\sigma}\rangle\rangle(\omega + i\delta) = \langle P^0_i\rangle \frac{1 - (\alpha^*_{\mathbf{k}})^2}{\omega - \varepsilon^*_{\mathbf{k}}} + \langle P^0_i\rangle \frac{(\alpha^*_{\mathbf{k}})^2}{\omega - (\varepsilon^*_f + \langle P^0_i\rangle \Delta^*_{\mathbf{k}})}. \quad (47)$$

The electronic structure can be made descriptive by evaluating the DOS of the c and f electrons. These quantities are given by $\rho_c(\omega) = -1/(\pi N)\sum_{\mathbf{k}} \mathrm{Im}\langle\langle c_{\mathbf{k}\sigma}; c^\dagger_{\mathbf{k}\sigma}\rangle\rangle(\omega + i\delta)$ and similarly for the f DOS. The results are shown in Figure 7 for the same system as in Figure 3. Here we have used Lorentzian broadening with a width of $s = 10^{-4}$. The DOS of the c electrons remains mainly flat as we expect from the constant DOS for the bare conduction electrons, but it shows a gap around the renormalised energy ε^*_f. On the other hand, the DOS of the f electrons increases sharply around the gap, meaning that there is a high DOS at the Fermi energy ($\mu = 1$). This picture qualitatively coincides with the electronic structure obtained from other approaches to the PAM, such as the SBMF theory, and conveys the idea of heavy quasiparticles. A remarkable difference to the SBMF result is an additional excitation peak in the upper band, which is due to the above discussed deformation of the quasiparticle bands (cf. Fig. 3). It possesses the character of a Van Hove-like singularity, as the DOS becomes very small in this energy range. This large DOS comes from the consideration of local fluctuations, which lead to a renormalisation of the f level. This can be contrasted to the case, in which we keep this energy constant during the flow process. With this assumption the quasiparticle bands coincide with those of the SBMF theory and do not show this type of excitation.

6 Conclusions

In this paper we have presented the description of heavy fermion behaviour within the framework of Wegner's flow equation method. This work provides a new semi-analytical approach to HFS. The basic idea of this scheme is the derivation of an effective Hamiltonian, that describes the essential physics of the system. Though this Hamiltonian is not diagonal in terms of usual fermion creation and destruction operators, it characterises two decoupled subsystems of electrons. Due to the Hubbard operators we have used for the f electrons, the according subsystem needs further approximations for the evaluation of physical properties, such as expectation values and correlation functions. In general, our findings confirm the picture that is provided by previous calculations, such as the SBMF theory. However, the flow equation approach to the PAM yields an additional excitation in the upper quasiparticle band and a significant decrease of the Kondo temperature.

In order to obtain a closed set of differential equations, we had to resort to a decoupling approximation, and we have only considered contributions in the leading order of ν_f. The idea of the second step is similar to the procedure used in the SBMF theory. However, in this context the two approaches cannot be compared in a one-to-one fashion. As we have seen in the discussion of

Section 5.1 an improvement of the present approximations can be obtained by an enhancement of the factorisation scheme due to the importance of charge fluctuations in the case of small degeneracy. An important difference of the flow equation approach to the SBMF theory is the determination of the energy ε_f^*. Whereas in the SBMF theory this energy is obtained by a mean field procedure and has to be determined self-consistently, the present method uses the integration of a differential equation. The procedure of self-consistency within the flow equation method only refers to expectation values. As we have shown in this paper, the differential equations can be solved both analytically and numerically. Though the first was performed on the basis of further simplifications, and it was intended to give a rough estimate, it turned out to coincide qualitatively good with the numerical solution. In accordance to the SBMF theory the present calculations show a restriction to parameter regimes where the occupation number of the f-sites is less than unity, as the solution breaks down in the limit $\langle P_i^0\rangle = 0$. However, we obtain good results for quite small deviations from this point. As we have stressed in Section 5.1 this breakdown is a result of the scheme of selfconsistency, while the integration of the flow equations is rather robust and shows a good convergence even in this limit.

In the present paper we studied the paramagnetic phase of the one-dimensional system. From recent works we know that the ground state of the KLM in one dimension is either ferromagnetic or non-ordered. On the other hand DMRG studies for the $U = \infty$ PAM also showed regions of short-range antiferromagnetism in the Kondo regime [17], whereas the ground state is found to be paramagnetic for the mixed-valent region. For the latter our results are consistent to those obtained in reference [17]. Near the Kondo regime magnetic interactions, such as the RKKY interaction, become more important. For a better understanding these contributions must be incorporated in the present scheme. Due to the semi-analytical character of the flow equation method we believe that this task could be accomplished for larger system sizes as usually considered in the DMRG. Another intriguing issue which was addressed in recent works about one-dimensional heavy fermion systems is the study of Luttinger liquid behavior [29]. However, this subject was merely discussed for the KLM and an occurence of a Luttinger liquid in the PAM is still an outstanding problem. The examination of this issue though needs a further enhancement of the calculations and cannot be obtained on a simple mean-field level.

Our findings for the excitation of the quasiparticles allow a clear distinction of c and f contributions. Generally, the electronic structure of the PAM comprises two quasiparticle bands, which are divided by a gap. The DOS is strongly enhanced at the Fermi level, resulting in quasiparticle masses up to several hundreds of bar electron masses. Such a behaviour characterises the experiments for heavy fermion compounds. In comparison to previous theoretical works on the PAM, the present paper shows an additional Van Hove-like excitation peak in the upper quasiparticle band, which is due to a significant flattening of the dispersion.

We also have investigated the dependence of the Kondo temperature on the hybridisation V^{i}. This quantity vanishes exponentially for small values of V^{i}. Our findings for T^* are consistent with the qualitative arguments proposed by Noziéres, suggesting a significant decrease of T^* compared to the Kondo temperature of the SIAM.

The author gratefully acknowledges K. Becker, R. Hetzel, T. Sommer and M. Vojta for fruitful discussions and helpful hints.

Appendix A: Decoupling scheme

Here we present the factorisation procedure discussed in Section 3.1 for the contributions in equation (14). With the denotations $\langle c^\dagger_{\mathbf{k}\sigma} c_{\mathbf{k}\sigma}\rangle = \langle n^c_{\mathbf{k}\sigma}\rangle$ and $\langle \hat f^\dagger_{i\sigma'} \hat f_{i\sigma}\rangle = \langle n^f_{i\sigma}\rangle$ we obtain

$$\begin{aligned}
&\frac{1}{N}\sum_{\mathbf{k}\mathbf{k}'}\sum_{i\sigma} e^{i(\mathbf{k}'-\mathbf{k})\mathbf{R}_i}\,\eta_{\mathbf{k}} V_{\mathbf{k}'}\, c^\dagger_{\mathbf{k}\sigma} c_{\mathbf{k}'\sigma} P_i^0 + \text{h.c.}\\
&\quad\longrightarrow 2\sum_{\mathbf{k}\sigma}\eta_{\mathbf{k}} V_{\mathbf{k}}\langle P_i^0\rangle\, c^\dagger_{\mathbf{k}\sigma} c_{\mathbf{k}\sigma} + \frac{2}{N}\sum_{i\mathbf{k}\sigma}\eta_{\mathbf{k}} V_{\mathbf{k}}\langle n^c_{\mathbf{k}\sigma}\rangle\, P_i^0\\
&\qquad - 2\sum_{\mathbf{k}\sigma}\eta_{\mathbf{k}} V_{\mathbf{k}}\langle P_i^0\rangle\,\langle n^c_{\mathbf{k}\sigma}\rangle \qquad\qquad (A.1)\\
&\frac{1}{N}\sum_{\mathbf{k}\mathbf{k}'}\sum_{i\sigma\sigma'} e^{i(\mathbf{k}'-\mathbf{k})\mathbf{R}_i}\,\eta_{\mathbf{k}} V_{\mathbf{k}'}\, c^\dagger_{\mathbf{k}\sigma} c_{\mathbf{k}'\sigma'} \hat f^\dagger_{i\sigma'} \hat f_{i\sigma} + \text{h.c.}\\
&\quad\longrightarrow 2\sum_{\mathbf{k}\sigma}\eta_{\mathbf{k}} V_{\mathbf{k}}\langle n^f_{i\sigma}\rangle\, c^\dagger_{\mathbf{k}\sigma} c_{\mathbf{k}\sigma} + \frac{2}{N}\sum_{i\mathbf{k}\sigma}\eta_{\mathbf{k}} V_{\mathbf{k}}\langle n^c_{\mathbf{k}\sigma}\rangle\, \hat f^\dagger_{i\sigma}\hat f_{i\sigma}\\
&\qquad - 2\sum_{\mathbf{k}\sigma}\eta_{\mathbf{k}} V_{\mathbf{k}}\langle n^f_{i\sigma}\rangle\,\langle n^c_{\mathbf{k}\sigma}\rangle. \qquad\qquad (A.2)
\end{aligned}$$

In order to obtain the appropriate contributions to the one-particle terms of the Hamiltonian from equation (A.1) it is convenient to make use of the relation $P_i^0 + \sum_\sigma \hat f^\dagger_{i\sigma}\hat f_{i\sigma} = \mathbf{1}$. The remaining interactions are decoupled as follows

$$\begin{aligned}
&\frac{1}{\sqrt{N}}\sum_{\mathbf{k}\sigma}\sum_{i\neq j}\eta_{\mathbf{k}} t_{ij} e^{-i\mathbf{k}\mathbf{R}_i} P_i^0 c^\dagger_{\mathbf{k}\sigma}\hat f_{j\sigma} + \text{h.c.}\\
&\qquad\longrightarrow \sum_{\mathbf{k}\sigma}\eta_{\mathbf{k}}\Delta_{\mathbf{k}}\langle P_i^0\rangle\big(c^\dagger_{\mathbf{k}\sigma}\hat f_{\mathbf{k}\sigma} + \hat f^\dagger_{\mathbf{k}\sigma} c_{\mathbf{k}\sigma}\big)\\
&\qquad\quad + \frac{1}{N}\sum_{i\mathbf{k}\sigma}\eta_{\mathbf{k}}\Delta_{\mathbf{k}}\langle A_{\mathbf{k}\sigma}\rangle P_i^0\\
&\qquad\quad - \frac{1}{N}\sum_{i\mathbf{k}\sigma}\eta_{\mathbf{k}}\Delta_{\mathbf{k}}\langle A_{\mathbf{k}\sigma}\rangle\,\langle P_i^0\rangle \qquad\qquad (A.3)
\end{aligned}$$

$$\frac{1}{\sqrt{N}}\sum_{\mathbf{k}\sigma\sigma'}\sum_{i\neq j}\eta_{\mathbf{k}}\,t_{ij}\,e^{-i\mathbf{k}\mathbf{R}_i}\hat{f}^\dagger_{i\sigma'}\hat{f}_{i\sigma}c^\dagger_{\mathbf{k}\sigma}\hat{f}_{j\sigma'}+\text{h.c.}$$
$$\longrightarrow\sum_{\mathbf{k}\sigma}\eta_{\mathbf{k}}\Delta_{\mathbf{k}}\langle n^f_{i\sigma}\rangle\big(c^\dagger_{\mathbf{k}\sigma}\hat{f}_{\mathbf{k}\sigma}+\hat{f}^\dagger_{\mathbf{k}\sigma}c_{\mathbf{k}\sigma}\big)$$
$$+\frac{1}{N}\sum_{i\mathbf{k}\sigma}\eta_{\mathbf{k}}\Delta_{\mathbf{k}}\langle A_{\mathbf{k}\sigma}\rangle\hat{f}^\dagger_{i\sigma}\hat{f}_{i\sigma}$$
$$-\sum_{\mathbf{k}\sigma}\eta_{\mathbf{k}}\Delta_{\mathbf{k}}\langle n^f_{i\sigma}\rangle\langle A_{\mathbf{k}\sigma}\rangle \tag{A.4}$$

where $\langle A_{\mathbf{k}\sigma}\rangle=\langle c^\dagger_{\mathbf{k}\sigma}\hat{f}_{\mathbf{k}\sigma}+\hat{f}^\dagger_{\mathbf{k}\sigma}c_{\mathbf{k}\sigma}\rangle$ was used.

Appendix B: Local expectation values

The expectation value $\langle P^0_i\rangle$ is best evaluated by making use of the the relation

$$P^0_i=\mathbf{1}-\sum_\sigma\hat{f}^\dagger_{i\sigma}\hat{f}_{i\sigma}. \tag{B.1}$$

Further we can take advantage of the translations invariance of the system, which allows us to write $\langle\hat{f}^\dagger_{i\sigma}\hat{f}_{i\sigma}\rangle=1/N\sum_j\langle\hat{f}^\dagger_{j\sigma}\hat{f}_{j\sigma}\rangle$. Consequently, it is convenient to regard the unitary transformation of the operator

$$F=1/N\sum_{i\sigma}\hat{f}^\dagger_{i\sigma}\hat{f}_{i\sigma}. \tag{B.2}$$

Its ℓ-dependence can be described in the usual way by $\mathrm{d}F(\ell)/\mathrm{d}\ell=[\eta(\ell),F(\ell)]$, where the generator is given by (10). Thus the following ansatz for the operator is expedient

$$F(\ell)=\frac{1}{N}\sum_{\mathbf{k}\sigma}\big(A^{(1)}(\ell)+A^{(2)}_{\mathbf{k}}(\ell)\big)\hat{f}^\dagger_{\mathbf{k}\sigma}\hat{f}_{\mathbf{k}\sigma}$$
$$+\frac{1}{N}\sum_{\mathbf{k}\sigma}B_{\mathbf{k}}(\ell)c^\dagger_{\mathbf{k}\sigma}c_{\mathbf{k}\sigma}$$
$$+\frac{1}{N}\sum_{\mathbf{k}\sigma}G_{\mathbf{k}}(\ell)\big(c^\dagger_{\mathbf{k}\sigma}\hat{f}_{\mathbf{k}\sigma}+\hat{f}^\dagger_{\mathbf{k}\sigma}c_{\mathbf{k}\sigma}\big)+\frac{E(\ell)}{N}. \tag{B.3}$$

In this connection the boundary condition $A^{(1)}(\ell=0)=1$ hold, whereas all the other coefficients are equal to zero for $\ell=0$. Evaluating the commutator we arrive at

$$[\eta,F]=-\frac{1}{N^2}\sum_{\mathbf{k}\sigma}\eta_{\mathbf{k}}\big(-B_{\mathbf{k}}+A^{(1)}+\langle P^0_i\rangle A^{(2)}_{\mathbf{k}}\big)$$
$$\times\ \big(c^\dagger_{\mathbf{k}\sigma}\hat{f}_{\mathbf{k}\sigma}+\hat{f}^\dagger_{\mathbf{k}\sigma}c_{\mathbf{k}\sigma}\big)$$
$$+\frac{1}{N}\sum_{i\mathbf{k}}\sum_{\sigma\sigma'}2\eta_{\mathbf{k}}G_{\mathbf{k}}\langle n^c_{\mathbf{k}\sigma}\rangle\hat{f}^\dagger_{i\sigma}\hat{f}_{i\sigma}$$
$$+\frac{1}{N}\sum_{\mathbf{k}\sigma}2\eta_{\mathbf{k}}G_{\mathbf{k}}\langle P^0_i\rangle c^\dagger_{\mathbf{k}\sigma}c_{\mathbf{k}\sigma}$$
$$-\frac{1}{N}\sum_{\mathbf{k}\sigma}2\eta_{\mathbf{k}}G_{\mathbf{k}}\hat{f}^\dagger_{\mathbf{k}\sigma}\hat{f}_{\mathbf{k}\sigma}$$
$$+\frac{1}{N^2}\sum_{\mathbf{k}i\sigma}2\eta_{\mathbf{k}}G_{\mathbf{k}}\langle n^c_{\mathbf{k}\sigma}\rangle\big(1-\langle P^0_i\rangle\big). \tag{B.4}$$

Here the decoupling approximation, which was discussed in Section 3.1 is already done. As a result we obtain a closed set of flow equations for the coefficients

$$\frac{\mathrm{d}A^{(1)}}{\mathrm{d}\ell}=-\frac{1}{N}\sum_{\mathbf{k}\sigma}2\langle n^c_{\mathbf{k}\sigma}\rangle\eta_{\mathbf{k}}G_{\mathbf{k}} \tag{B.5}$$
$$\frac{\mathrm{d}A^{(2)}}{\mathrm{d}\ell}=-2\eta_{\mathbf{k}}G_{\mathbf{k}} \tag{B.6}$$
$$\frac{\mathrm{d}B_{\mathbf{k}}}{\mathrm{d}\ell}=2\langle P^0_i\rangle\eta_{\mathbf{k}}G_{\mathbf{k}} \tag{B.7}$$
$$\frac{\mathrm{d}G_{\mathbf{k}}}{\mathrm{d}\ell}=-\big(B_{\mathbf{k}}-A^{(1)}-\langle P^0_i\rangle A^{(2)}_{\mathbf{k}}\big)\eta_{\mathbf{k}} \tag{B.8}$$
$$\frac{\mathrm{d}E}{\mathrm{d}\ell}=\sum_{\mathbf{k}\sigma}2\eta_{\mathbf{k}}G_{\mathbf{k}}\langle n^c_{\mathbf{k}\sigma}\rangle\big(1-\langle P^0_i\rangle\big). \tag{B.9}$$

The following exact relations can be derived

$$A^{(1)}=1+\frac{1}{N}\sum_{\mathbf{k}\sigma}\langle n^c_{\mathbf{k}\sigma}\rangle A^{(2)}_{\mathbf{k}} \tag{B.10}$$
$$A^{(2)}_{\mathbf{k}}=-\frac{B_{\mathbf{k}}}{\langle P^0_i\rangle} \tag{B.11}$$
$$E=N\big(1-\langle P^0_i\rangle\big)\big(1-A^{(1)}\big). \tag{B.12}$$

Furthermore the differential equation

$$\langle P^0_i\rangle\frac{\mathrm{d}G^2_{\mathbf{k}}}{\mathrm{d}\ell}+\frac{\mathrm{d}B^2_{\mathbf{k}}}{\mathrm{d}\ell}-A^{(1)}\frac{\mathrm{d}B_{\mathbf{k}}}{\mathrm{d}\ell}=0 \tag{B.13}$$

holds. As a simplification we regard the summation on the right hand side of (B.10) a small correction, and we neglect it. Such an approximation is well confirmed by numerical simulations. As a consequence we obtain $A^{(1)}=1$ for the entire flow, and the differential equation (B.13) can be integrated straightforward

$$\frac{\mathrm{d}}{\mathrm{d}\ell}\arcsin\big[1-2B_{\mathbf{k}}\big]=-2\sqrt{\langle P^0_i\rangle}\eta_{\mathbf{k}}. \tag{B.14}$$

With the help of the unitarity relation (25) and (26) we can identify $B_{\mathbf{k}}=\langle P^0_i\rangle\beta^2_{\mathbf{k}}$, and the expectation value thus reads

$$\langle P^0_i\rangle=1-{}^*\langle F^*\rangle^*$$
$$=1-\frac{1}{N}\sum_{\mathbf{k}\sigma}\Big[\big(1-(\alpha^*_{\mathbf{k}})^2\big)\ {}^*\langle c^\dagger_{\mathbf{k}\sigma}c_{\mathbf{k}\sigma}\rangle^*$$
$$+\big(1-(\beta^*_{\mathbf{k}})^2\big)\ {}^*\langle\hat{f}^\dagger_{\mathbf{k}\sigma}\hat{f}_{\mathbf{k}\sigma}\rangle^*\Big]. \tag{B.15}$$

An equivalent procedure can be used in order to derive the expectation values $\langle c^\dagger_{\mathbf{k}\sigma}c_{\mathbf{k}\sigma}\rangle$ and $\langle A_{\mathbf{k}\sigma}\rangle$. Due to their nonlocal character the results coincide with those obtained in Section 3.1. Therefore it is more reasonable to use the single operator transformation, because this approach can be used to describe correlation functions, as pointed out in Section 5.4.

References

1. A.C. Hewson, *The Kondo Problem to Heavy Fermions*, 1st edn. (Cambridge University Press, Cambridge, 1993)
2. S. Kondo, D.C. Johnston, C.A. Swenson, F. Borsa, A.V. Mahajan, L.L. Miller, T. Gu, A.I. Goldman, M.B. Maple, D.A. Gajewski et al., Phys. Rev. Lett. **78**, 3729 (1997)
3. J. Hopkinson, P. Coleman, Phys. Rev. Lett. **89**, 267201 (2002)
4. F. Wegner, Ann. Phys. **3**, 77 (1994)
5. S. Glazek, K. Wilson, Phys. Rev. D **48**, 5863 (1993)
6. I. Grote, F. Wegner, J. Low Temp. Phys. **126**, 1385 (2000); V. Hankevych, I. Grote, F. Wegner, Phys. Rev. B **66**, 094516 (2002); V. Hankevych, F. Wegner, Eur. Phys. J. B **31**, 333 (2003)
7. P. Coleman, Phys. Rev. B **29**, 3035 (1984); P. Coleman, Phys. Rev. B **35**, 5072 (1987); D.M. Newns, N. Read, Adv. Phys. **36**, 799 (1987)
8. T.M. Rice, K. Ueda, Phys. Rev. Lett. **55**, 995 (1985); T.M. Rice, K. Ueda, Phys. Rev. B **34**, 6420 (1986)
9. G. Kotliar, A.E. Ruckenstein, Phys. Rev. Lett. **57**, 1362 (1986)
10. W. Metzner, D. Vollhardt, Phys. Rev. Lett. **62**, 324 (1989); A. Georges, G. Kotliar, W. Krauth, M.J. Rozenberg, Rev. Mod. Phys. **68**, 13 (1996)
11. T. Pruschke, R. Bulla, M. Jarrell, Phys. Rev. Lett. **61**, 12799 (2000)
12. A.N. Tahvildar-Zadeh, M. Jarrell, J.K. Freericks, Phys. Rev. Lett. **80**, 5168 (1998)
13. N.S. Vidhyadhiraja, A.N. Tahvildar-Zadeh, M. Jarrell, H.R. Krishnamurthy, Europhys. Lett. **49**, 459 (2000)
14. K. Tsutsui, Y. Ohta, R. Eder, S. Maekawa, E. Dagotto, J. Riera, Phys. Rev. Lett. **76**, 279 (1996)
15. C. Gröber, R. Eder, Phys. Rev. B **59**, 10405 (1999)
16. For a recent review see: H. Tsunetsugu, M. Sigrist, K. Ueda, Rev. Mod. Phys. **69**, 809 (1997)
17. M. Guerrero, R.M. Noack, Phys. Rev. B **53**, 3707 (1995); M. Guerrero, R.M. Noack, Phys. Rev. B **63**, 144423 (2001)
18. K.W. Becker, A. Hübsch, T. Sommer, Phys. Rev. B **66**, 235115 (2002)
19. in case we apply Wegner's choise for the generator, namely $\eta = [H_0, H_1]$, the flow parameter ℓ has the dimension of an inverse energy squared
20. C. Knetter, G. Uhrig, Eur. Phys. J. B **13**, 209 (2000)
21. S. Kehrein, A. Mielke, Ann. Phys. **252**, 1 (1996)
22. S. Kehrein, A. Mielke, P. Neu, Z. Phys. B **99**, 269 (1996)
23. here we have again neglected contributions of order ν_f^{-1}
24. A.A. Abrikosov, L.P. Gorkov, I.E. Dzyaloshinski, *Methods of the Quantum Field Theory in Statistical Physics*, 1st edn. (Dover Publications, New York, 1963)
25. P. Fulde, *Electron Correlations in Molecules and Solids*, Springer Series in Solid State Sciences, 2nd edn. (Springer-Verlag, Berlin, Heidelberg, New York, 1993)
26. K. Meyer, Ph.D. thesis (German), Dresden University of Technology (2003), URL=`http://hsss.slub-dresden.de/hsss/servlet/hsss.urlmapping.MappingServlet?id=1079709122000-4690`
27. K. Wilson, Rev. Mod. Phys. **47**, 773 (1975)
28. P. Nozières, Ann. Phys. (Paris) **10**, 19 (1985); P. Nozières, Eur. Phys. J. B **6**, 447 (1998)
29. N. Shibata, A. Tsvelik, K. Ueda, Phys. Rev. B **56**, 330 (1997)